Turk J Elec Eng & Comp Sci, Vol.18, No.1, 2010, © TÜBİTAK
doi:10.3906/elk-0812-5

Adaptive hysteresis band control for constant switching frequency in DTC induction machine drives

H. İbrahim OKUMUŞ, Mustafa AKTAŞ
Department of Electrical & Electronics Engineering
Karadeniz Technical University, Faculty of Engineering
61080 Trabzon-TURKEY
e-mail: okumus@ktu.edu.tr, maktas@ktu.edu.tr

Abstract

It is fairly well known that direct torque control (DTC) exhibits fast dynamic torque response, a property that originates in the fact that torque and flux is directly controlled by instantaneous space voltage vector, unlike field-oriented control. For this reason direct torque control gradually has been used in the field, eliciting quick response and high efficiency since its introduction in the mid-1980s. Conventional fixed band hysteresis control has several problems. One of these is variable switching frequency, which causes serious problems in DTC. In this paper, an adaptive hysteresis band control strategy is proposed, where the hysteresis band is controlled in real time as variation of applied voltage vectors, thereby reducing the torque ripple whilst maintaining a constant torque switching frequency. The proposed adaptive hysteresis band control technique is verified by simulations. The system is first simulated by using the program Matlab and tested by hardware in the loop. Then, it is implemented in hardware based on a TMS320C6711, 32-bit fixed-point digital signal processor. Experimental results prove the feasibility of the proposed strategy compared with conventional method.

Key Words: *Constant switching frequency, direct torque control, induction machine drive, torque ripple.*

1. Introduction

Technological advances in power semiconductor and microprocessor technology have made possible the application of advanced control techniques to ac motor drives [1]. Presently, direct torque control (DTC) is the most advanced AC drive technology, as it provides fast dynamic torque response and robustness to machine parameter variations without the use of current regulators. The technique can be easily implemented using two hysteresis controllers (one for flux, one for torque) and a switching table to select the switching voltage vector. However, a conventional DTC suffers from effects such as torque ripple, variable switching frequency and flux drooping at low speed. These effects result in increased sub-harmonic currents, higher load current ripple and variable switching losses in the inverter [2, 3].

The variation in switching frequency, due to fixed band hysteresis torque and flux controllers, is a limitation of the conventional DTC scheme as originally mentioned in [4]. In the literature, various techniques have been proposed to solve this problem, including the use of variable hysteresis bands [3], predictive control schemes [5], space vector modulation techniques [6] and intelligent control methods [7]. Torque controllers which produce constant torque switching frequency have been investigated in [8–10]. The technique replaces the conventional hysteresis torque controller with a constant switching frequency controller. Subsequently, an almost fixed switching frequency is obtained by comparing the triangular waveforms with the compensated torque error signal.

This paper proposes an adaptive hysteresis band control strategy, where the hysteresis band is controlled in real time via variation of applied voltage vectors, by which the torque ripple is reduced while maintaining constant torque switching frequency.

2. Direct torque control principles

In general, in a symmetrical three-phase induction machine, an instantaneous electromagnetic torque is a cross-product of the stator and rotor flux linkage space vector or stator current space vector and stator flux linkage space vector:

$$T_e = \frac{3}{2} P \bar{\Psi}_s \times \bar{I}_s. \tag{1}$$

Here, $\bar{\Psi}_s$ is the stator flux linkage space vector and $\bar{I}_s$ is the stator space vector. In equation (1), both space vectors are expressed in the stationary reference frame. By considering that $\bar{\Psi}_s = L_s \bar{I}_s + L_m \bar{I}'_r$, $\bar{\Psi}'_r = L_r \bar{I}_r + L_m \bar{I}_s$, where the primed rotor quantities are expressed in the stationary reference frame, it follows that $\bar{I}_s = \bar{\Psi}_s / L'_s - [L_m/(L_r L'_s)]\, \bar{\Psi}'_r$. Thus, equation (1) takes the form

$$T_e = \frac{3}{2} P \frac{L_m}{L'_s L_r} \left|\bar{\Psi}'_r\right| \left|\bar{\Psi}_s\right| \sin\gamma. \tag{2}$$

The electromagnetic torque given by equation (2) is a sinusoidal function of γ, the angle between the stator and rotor flux linkage space vector. The magnitude of the stator flux is normally kept constant and the motor torque controlled by means of the angle γ. The rotor time constant of the standard induction machine is typically larger than 100 ms; thus the rotor flux is stable and variations in the rotor flux are slow compared with the stator flux. It is therefore possible to achieve the required torque very effectively by rotating the stator flux vector directly in a given direction as fast as possible.

Figure 1 shows stator flux behaviour compared to rotor flux, after a step variation stator pulsation, $\omega_{s0} = \omega_{s0} + \Delta\omega_s$, where ω_{s0} is the initial pulsation and $\Delta\omega_s$ is the step variation. Controlling the stator flux and electromagnetic torque control, achieved by using the appropriate stator voltages, can quickly change the electromagnetic torque. Choosing suitable voltage vectors, those increases or decreases to γ causes the electromagnetic torque to, in turn, increase or to decrease [11].

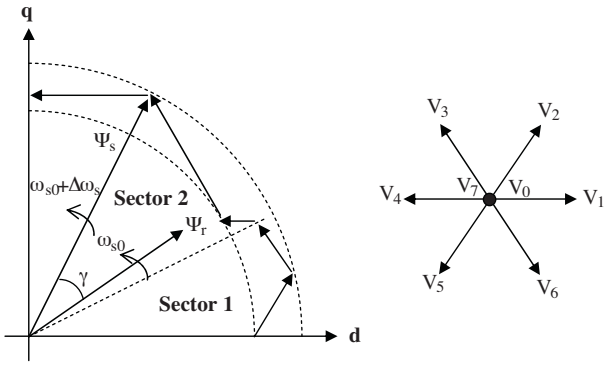

Figure 1. Optimum voltage vector in the torque control and voltage vectors.

The core of the system consists of a flux and torque estimator, a speed controller, a flux controller, a torque controller and an optimum switching Table 1. The estimator estimates the actual stator flux and torque by using two measured motor stator phase currents, the dc voltage and states of the power switches. Torque and flux references are compared with the actual values and a two-level for flux, and a three-level for torque hysteresis control method produces control signals.

Table 1. Switching table.

$d\psi$	dt_e	sector 1	sector 2	sector 3	sector 4	sector 5	sector 6
1	1	V_2	V_3	V_4	V_5	V_6	V_1
	0	V_7	V_0	V_7	V_0	V_7	V_0
	-1	V_6	V_1	V_2	V_3	V_4	V_5
0	1	V_3	V_4	V_5	V_6	V_1	V_2
	0	V_0	V_7	V_0	V_7	V_0	V_7
	-1	V_5	V_6	V_1	V_2	V_3	V_4

3. Hysteresis band control in DTC

The hysteresis band control method is a simple and common form of closed-loop control. The block diagrams for the two-level and three-level hysteresis band control methods are shown in Figures 2 and 3. Hysteresis band control is widely used because of its ability to be simply implemented. Besides the fast response, the inherent peak current limiting capability and excellent dynamic performance that it offers, it does not require an accurate knowledge of the load parameters. In addition, hysteresis band control is essentially an analog technique. Despite the advantages given by the digital controllers, in terms of interfacing, maintenance, flexibility, and integration, their accuracy and response speed are often insufficient for current control in highly demanding applications, such as active filters and high precision drives. In a DTC scheme, the objective is to reduce both the stator flux and torque errors to zero using hysteresis comparators select the optimum voltage vector.

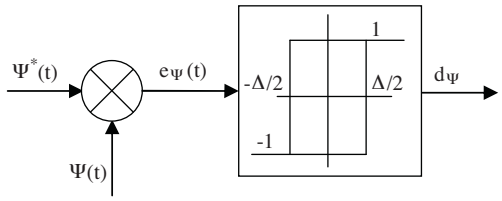

Figure 2. Block diagram of two-level Hysteresis Band Control.

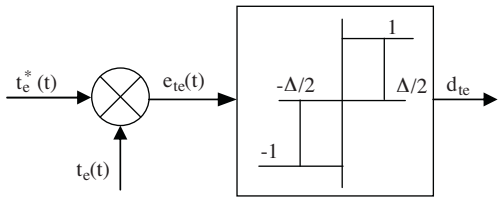

Figure 3. Block diagram of three-level Hysteresis Band Control.

Hysteresis comparators lie at the heart of DTC schemes and are responsible not only for determining the optimum voltage vector to be switched, but also for determining how long that vector or action remains selected. Hysteresis is used to prevent the power devices from switching unnecessarily at each new update or switching decision.

In this study, a two level hysteresis comparator, as shown in Figure 2, is used in the DTC to compare the actual value of stator flux to the internal reference value produced by stator flux reference controller. In the similar manner, a three level hysteresis comparator, as shown in Figure 3, is used to compare the actual value of the torque to the internal reference value produced by the speed torque reference controller [11]. The outputs of these comparators update every sampling time and they indicate whether the flux or torque must be varied.

4. Adaptive hysteresis band strategy

In a DTC scheme, for fixed torque band amplitude ΔT_e, the inverter switching frequency is related to the amplitude of the flux hysteresis band $\Delta\Psi$. A small flux hysteresis bandwidth results in a higher switching frequency, the stator flux vector locus approaches a circle and the phase current waveform is nearly sinusoidal. These operating conditions result in low harmonic copper losses in the machine while switching losses in the inverter are high. Alternatively, a large hysteresis bandwidth for stator flux decreases the switching frequency and the stator flux vector locus becomes a hexagon. In this case, switching losses decrease in the inverter while the harmonic copper losses increase in the machine [12].

Adaptive hysteresis band has been well investigated as a two level strategy. The adaptive hysteresis band strategy can be extended to three level hysteresis band. It is demonstrated that adapting the width of the hysteresis band for the three level strategy as a function of pulse number FR and depth M. The block diagram of three level hysteresis band to be analysed is illustrated in Figure 4. Output $t_e(t)$ tracks the reference function $t_e^*(t)$ to within a band whose limit is $\Delta + \Sigma$. It is important to note that Σ is required only to create the three voltage level in the output of the hysteresis element. In simulation results Σ is decrease down a very small value and for the simulation results presented in this paper it was set to be $\Delta/100$.

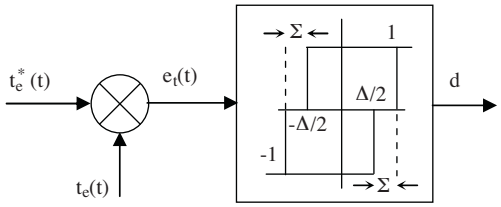

Figure 4. Block diagram of three level adaptive hysteresis band control.

Adaptive hysteresis band is inherently an analogue process because switching is produced at the intersection of the error between $t_e^*(t)$ and $t_e(t)$ and the adaptive hysteresis band limits. The equations describing these intersection points are nonlinear and transcendental and therefore must be solved off-line:

$$p = \frac{\left[\left(t_e(t_2) + \frac{\Delta}{2}\right) - \left(t_e(t_1) - \frac{\Delta}{2}\right)\right]}{t_2 - t_1} \tag{3}$$

The following analysis illustrates the pulse-position that occurs in three-level adaptive hysteresis band control. The production of one pulse for the three-level adaptive hysteresis band control method is illustrated in Figure 5. By inspection of Figure 5, the slope of the signal $t_e(t)$ when the output is $+V/2$ can be described as in equation (3). It is necessary to assume a fixed slope for the reference function to describe the adaptive hysteresis band process as a continuous function of time. This assumption has not been found to produce significant errors in the switching angles using the analogue simulation [12]. By assuming a fixed gradient of $t_e(t)$ over each switching period, the "on"- or $t_2 - t_1$ time can be approximated as

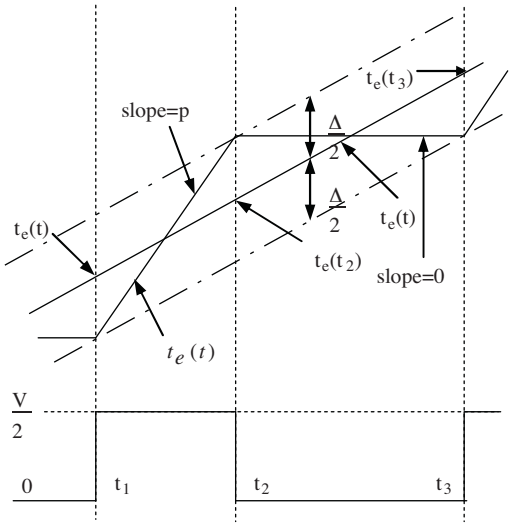

Figure 5. Production of one pulse for three level adaptive hysteresis band control.

$$t_{on} = \frac{\Delta}{p - t_e'(t)}. \tag{4}$$

The slope of output signal $\hat{t}_e(t)$ during the time $t_2 < t < t_3$ is zero because the output voltage is zero in this time period. Therefore from inspection of Figure 5, the slope of the reference function can be expressed as

$$t_e'(t) \approx \frac{t_e(t_3) - t_e(t_2)}{t_3 - t_2} = \frac{\Delta}{t_3 - t_2} \tag{5}$$

and therefore the corresponding off time may be expressed as

$$t_{off} = t_3 - t_2 = \frac{\Delta}{t_e'(t)}. \tag{6}$$

By combining equations (4) and (6), the total instantaneous time period T_i is described as

$$T_i = t_{on} + t_{off} = \frac{\Delta}{p - t'_e(t)} + \frac{\Delta}{t'_e(t)}. \tag{7}$$

The corresponding instantaneous angular frequency ω_i is determined by

$$\omega_i = \frac{2\pi}{T_i}. \tag{8}$$

The carrier frequency ω_c, which determines the pulse number, is the average value of the instantaneous frequency ω_i over one fundamental period and is expressed as

$$\omega_c = \frac{2}{\Delta p}\left[2A\omega p - \frac{A^2\omega^2\pi}{2}\right]. \tag{9}$$

The analysis presented demonstrates that the pulse number FR is a function of reference function amplitude A, slope p, the output signal $\hat{t}_e(t)$, and the width of the hysteresis band, Δ. Therefore, it is necessary to adapt the width of the hysteresis band so that it has a constant width along a fundamental period according to equation (10). This enable only the pulse number FR and depth M to be the specified parameters in the modulation process [12]. Therefore, the width of the adaptive hysteresis band can be expressed as

$$\Delta = \frac{4Mp}{\omega_c}\left[1 - \frac{M\pi}{4}\right], \tag{10}$$

where $\omega_c = FR\omega$ and the depth M is defined as

$$M = \frac{A\omega}{p}. \tag{11}$$

5. Simulation and experimental results

Simulation and experimental results presented confirm the theoretical analysis. A brief description of the simulation and experimental set-up are given. Comparisons between conventional hysteresis based torque controller and the proposed adaptive hysteresis based torque controller using the simulation and experimental results are presented.

5.1. Simulation results

A simulation study for the proposed adaptive hysteresis band control technique was carried out using the MATLAB software package. The motor parameters used in the simulations are given in Table 2.

The average inverter switching frequency f_s is defined as $f_s = N_s/T_f$, where N_s is the number of switching operations for one leg of the inverter in one fundamental period and T_f is the fundamental period. To calculate the average inverter switching frequency f_s experimentally, a simple program written in C is developed and inserted in the service routine of the DSP program. The number of switching operations for a single inverter leg over a fundamental period is calculated and then divided by the fundamental period. The

average inverter switching frequency is also calculated by computer simulation using the MATLAB software package. The graphical variations of the average inverter switching frequencies for five different rotor speeds are illustrated in Figure 6.

Table 2. Parameters of Induction Motor and Settings.

Power, P_N	0.37 kW
Frequency, f_N	50 Hz.
Supply Voltage (Delta/Star cont.) CCCon	0–240 V / 380–415 V
Line current, I_N (Delta/Star cont.)	1.9/1.1 A
Pole pairs, P	2
Stator resistance, R_s	28.13 Ω
Rotor resistance, R_r	20.76 Ω
Stator self inductance, L_s	0.634 H
Rotor self inductance, L_r	0.634 H
Mutual inductance, M	0.4226 H
Inertia, J	0.002 kg.m^2

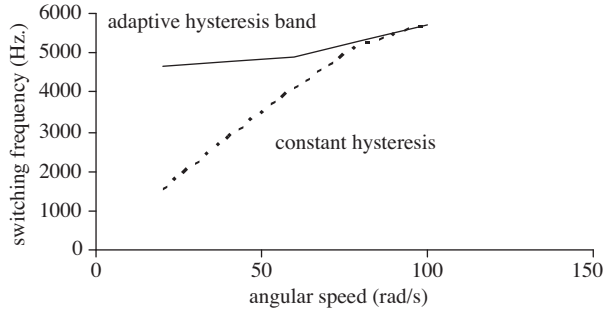

Figure 6. Variation of switching frequency for different rotor speeds.

It can be seen from the graphic that there is large variation in the average switching frequency between rotor speeds of 10 rad/s and 100 rad/s, with the conventional hysteresis based torque controller. The proposed torque controller, however, has a significantly smaller variation when compared to the conventional controller.

In the simulation, the proposed DTC drive is operated in the speed control mode with a stator flux and a rotor speed references of 0.8 Wb and 200 rad/s, respectively. Figure 7 shows the simulation results for the stator flux locus, the steady-state stator phase flux and switching frequency. From the figure, it is observed that the flux locus in Figure 7(b) is circular while the flux locus in Figure 7(a) looks like a hexagon. It should be noted that the effect of the proposed scheme can be seen very easily from the simulation results. The advantages of the proposed controller are less torque ripple and safer switching for power switches.

5.2. Experimental results

The experimental set-up of the proposed DTC motor drive system is shown in Figure 8. The setup consist of a 0.37 kW cage-rotor induction machine; an IGBT inverter; a Texas Instruments 200 MHz, TMS320C6711 DSP; and a 200 kHz, ADS8364 EVM ADC board. Figure 9 shows the steady-state stator flux locus. It is clear that the stator flux ripple significantly becomes less with the proposed controller. Also, the corresponding steady-state stator flux and electromagnetic torque response are shown in Figures 10 and 11, respectively.

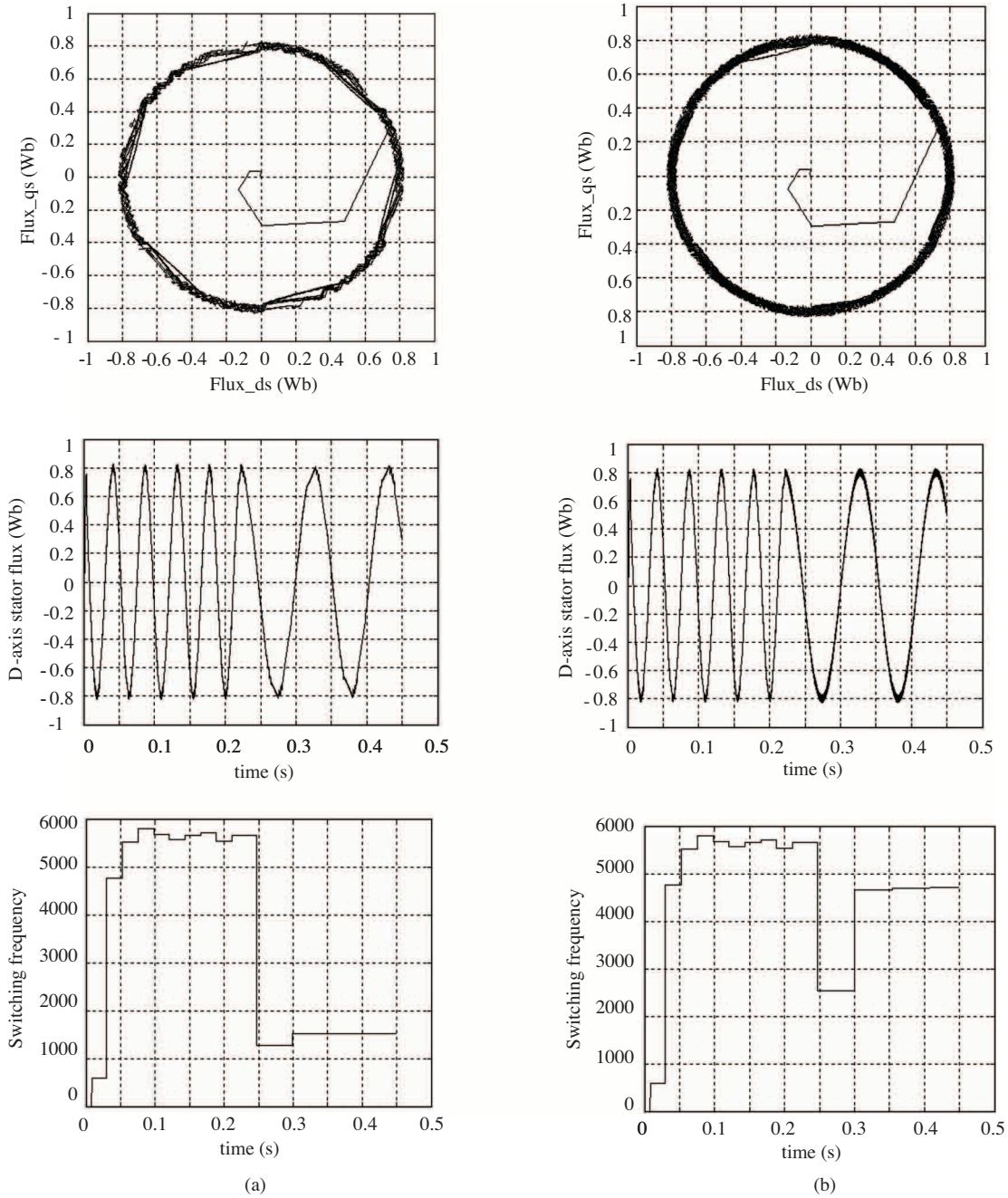

Figure 7. Simulation results of stator flux locus, steady-state phase flux and switching frequency, (a) conventional hysteresis-based torque and flux controllers, (b) proposed adaptive hysteresis-based torque and conventional hysteresis-based flux controllers.

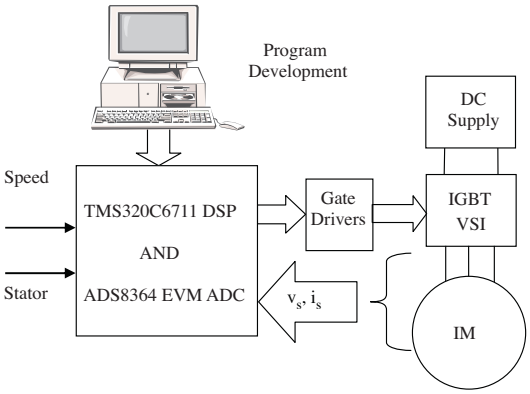

Figure 8. Experimental setup.

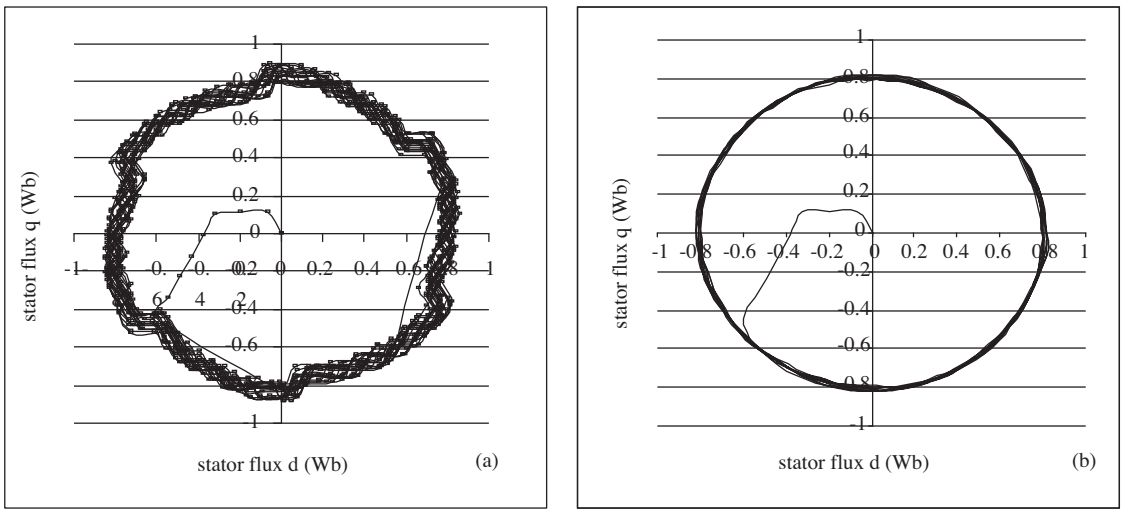

Figure 9. Experimental stator flux locus for (a) conventional hysteresis-based torque and flux controllers, (b) proposed adaptive hysteresis-based torque and conventional hysteresis-based flux controllers.

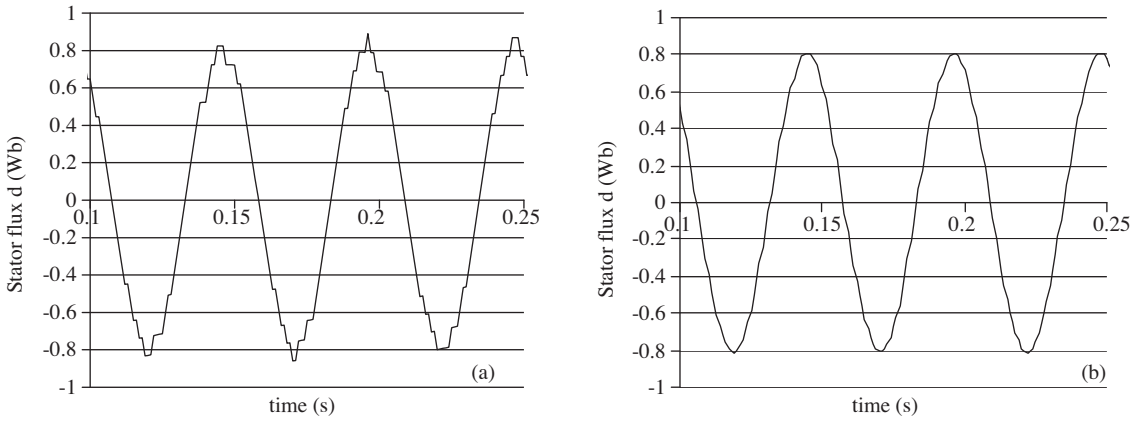

Figure 10. Experimental results of steady-state stator phase flux, (a) conventional hysteresis-based torque and flux controllers, (b) proposed adaptive hysteresis-based torque and conventional hysteresis-based flux controllers.

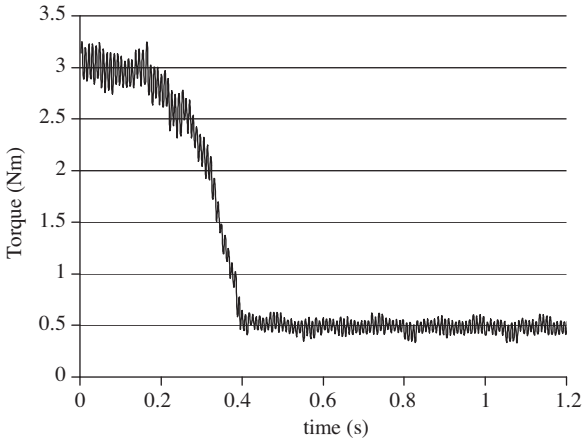

Figure 11. Experimental result of electromagnetic torque for proposed strategy.

6. Conclusions

This paper presents an adaptive hysteresis band control strategy, where the hysteresis band is controlled in real time as variation of applied voltage vectors. Thereby the torque ripple is reduced whilst maintaining a constant torque switching frequency.

The proposed methods are investigated using a TMS320C6711 DSP, IGBT voltage supply inverter and three-phase induction motor. The simulation studies and the experimental results have been compared. As a consequence, it is seen that the results of both studies support each other.

The proposed control technique is verified by simulation and experimental results. With the proposed technique, the switching frequency of the inverter is nearly held constant.

References

[1] Bose Bimal K., An Adaptive Hysteresis-Band Current Control Technique of a Voltage-Fed PWM Inverter for Machine Drive System, IEEE Trans. Industrial Electronics, Vol 37, pp. 402-408, Oct. 1990

[2] Casadei D, Grandi G, Serra G, Effects of Flux and Torque Hysteresis Band Amplitude in Direct Torque Control of Induction Machines, IECON'94, Bologna, Italy, pp.299-304, 5-9 September 1994.

[3] J.K.Kang, D.W. Chung, S.K. Sul, Direct Torque Control of Induction Machine With Variable Amplitude Control of Flux and Torque Hysteresis Bands, IEEE/IEMD Int.Conf., pp. 640-642, 1999

[4] I. Takahashi, T. Noguchi, A New Quick-Response and High-Efficiency Control Strategy of an Induction Motor, IEEE Trans. Industry App. IA-22, pp. 820-827, 1986.

[5] Y. Li, J. Shao, and B. Si, "Direct torque control of induction motors for low speed drives considering discrete effect of control and dead-time timing of inverters," in *Proc. IEEE-IAS Annu. Meeting*, 1997, pp. 781–788.

[6] L. Tan and M. F. Rahman, "A new direct torque control strategy for flux and torque ripple reduction for induction motors drive by using space vector modulation," in *Proc. 32nd Annu. PESC*, 2001, vol. 3, pp. 1440–1445.

[7] S. Mir and M. E. Elbuluk, "Precision torque control in inverter-fed induction machines using fuzzy logic," in *Proc. IEEE-IAS Annu. Meeting*, 1995, pp. 396–401.

[8] N. R. N. Idris and A. H. M. Yatim, "Reduced torque ripple and constant torque switching frequency strategy for Direct Torque Control of induction machine," in *Proc. 15th IEEE-APEC*, New Orleans, LA, 2000, pp. 154–161.

[9] N. R. N. Idris and A. H. M. Yatim, "Direct torque control of induction machines with constant switching frequency and reduced torque ripple," *IEEE Trans. Ind. Electron.*, vol. 51, no. 4, pp. 758–767, Aug. 2004.

[10] C. L. Toh, N. R. N. Idris, and A. H.M. Yatim, "Constant and high switching frequency torque controller for DTC drives," *IEEE Power Electron. Lett.*, vol. 3, no. 2, pp. 76–80, Jun. 2005.

[11] Okumus H. I., Improved Direct Torque Control of Induction Machine Drives Phd Thesis, UNIVERSITY OF BRISTOL, UK, July 2001

[12] Bowes S.R, Grewal S, Three-level hysteresis band modulation strategy for single-phase PWM inverter, IEEE Proc.-Electr. Power Appl., Vol. 146, No 6, November 1999.